Zachara John M. (Orcid ID: 0000-0002-9883-7874)

Chen Xingyuan (Orcid ID: 0000-0003-1928-5555)

Song Xuehang (Orcid ID: 0000-0003-4932-595X)

Shuai Pin (Orcid ID: 0000-0003-2511-9828)

Kilometer-scale hydrologic exchange flows in a gravel-bed river corridor and their implications to solute migration

John M. Zachara[1*], Xingyuan Chen[1], Xuehang Song[1], Pin Shuai[1], Chris Murray[1], and C. Tom Resch[1]

[1]Pacific Northwest National Laboratory, Richland, WA

Submission to: *Water Resources Research*

Key Points: (140 characters max)

- River water exchange in gravel-bed river corridors may create a wide hyporheic zone.
- River water intrusion causes periods of variable groundwater flow directions, velocities, and compositions, and influences plume behavior.
- The residence time and transport distance of intruded river water is controlled by river stage and subsurface hydrogeologic features.

Correspondence

John Zachara, Pacific Northwest National Laboratory, Richland, WA; Phone (509) 371-6355;

Fax (509) 371-6354; E-mail: john.zachara@pnnl.gov

Abstract

A well-characterized field site along a major, gravel-bed river corridor was used to investigate the dynamic pathways and impacts of subsurface hydrogeologic structure on kilometer-scale hydrologic exchange flows between river water and groundwater. An aqueous uranium (U_{aq}) plume exists within a hyporheic alluvial aquifer at the site that discharges to the Columbia River. We performed temporally intensive monitoring of specific conductance (SpC) and U_{aq} concentrations within the plume for a two-year period at varying distances from the river shoreline, both within and outside a presumed subsurface pathway of lateral hydrologic exchange. Specific conductance and U_{aq} were utilized as in-situ tracers of hydrologic exchange and associated groundwater-surface water mixing. Seasonal river stage variations by more than 2 m caused distinct events of river water intrusion and retreat from the near-shore, hyporheic alluvial aquifer, resulting in highly dynamic SpC and U_{aq} patterns in monitoring wells. Simulations of hydrologic exchange and mixing were performed with PFLOTRAN to understand the observed SpC and U_{aq} behaviors linked to predominant flow directions and velocities in the river corridor as influenced by river stage dynamics and variable aquitard topography. By coupling robust monitoring with numerical flow and transport modeling, we demonstrate complicated multidirectional flow behaviors at the kilometer scale that strongly influenced plume dynamics. Therefore, hyporheic aquifer must be frequently monitored under different flow conditions if water quality is of concern. The resulting hydrologic understanding enables improved interpretation of hydrogeochemical data from this site and other large gravel-bed river corridors in the U.S. and elsewhere.

Index Terms (5):

- 1829 Groundwater hydrology
- 1830 Groundwater/surface water interaction

- 1847 Modeling
- 1856 River channels
- 1872 Time series analysis

Keywords:

- Surface water – groundwater interaction
- Gravel-bed river corridor
- Hydrologic exchange
- Subsurface hydrogeologic structures
- Riverine and groundwater modeling
- Contaminant plume dynamics

1. Introduction

The lateral, bidirectional exchange of water between rivers and associated subsurface waters is a process of fundamental significance in river corridor systems (Harvey, 2016; Harvey & Gooseff, 2015; Hauer et al., 2016; Malard et al., 2002). Hydrologic connectivity can occur well beyond the riverbed hyporheic zone, extending to the river bank (Harvey, 2016; Li et al., 2008; Unland et al., 2014) and/or hyporheic alluvial aquifers (Hauer et al., 2016) depending on hydraulic gradients and hydraulic conductivity field. Hydrologic exchange can enhance the biogeochemical transformation of nutrients and contaminants by facilitating contact of river water with reactive and microbiologically active subsurface sediments; relieving nutrient limitations through groundwater-surface water mixing (Harvey, 2016; Harvey et al., 2018; Shuai et al., 2017; Wondzell, 2015); and creating hot spots of biogeochemical activity at points of favorable thermal and/or nutrient conditions (Boulton et al., 2010; Gu et al., 2012; McClain et al., 2003). Thus, hydrologic exchange plays a critical

role in riverine ecological function; supporting biodiversity and primary productivity, nutrient transformations and cycling, and beneficial ecosystem services (Boulton et al., 2010; Brunke & Gonser, 1997; Dent et al., 2001; Harvey et al., 2018; Malard et al., 2002; Stanford et al., 2005; Stanford & Ward, 1993).

Hydrologic exchange beyond the riverbed is most prevalent in gravel-dominated riverine systems exhibiting coarse-textured sediments with high hydraulic conductivity, large seasonal discharge variations or managed flows for hydropower generation, and hydraulically-connected alluvial groundwater with low hydrologic gradient (Gerecht et al., 2011; Harvey, 2016; Hauer et al., 2016; Rosenberry et al., 2013; Sawyer et al., 2009; Siergieiev et al., 2015; Zachara et al., 2016; Zachara et al., 2013). Lateral hydrologic exchange occurs through intrusion of river water into river bank sediments during periods of high river stage, and the subsequent retreat or drainage of these stored waters as river discharge falls (Chen & Chen, 2003; Datry et al., 2008; Harvey, 2016; Liang et al., 2018; McCallum et al., 2010; Sophocleous, 2002; Unland et al., 2015). These exchanges cause rise in the groundwater table and the creation of domains of groundwater flow reversal, transient storage, and groundwater-surface water mixing (Boano et al., 2014; Hauer et al., 2016; Heeren et al., 2014; Heeren et al., 2011) that may strongly influence river corridor water composition, temperature, and oxygen saturation (Harvey et al., 2018; Helton et al., 2012; Valett et al., 2014). In some cases, hyporheic corridor flow may result where intruded river waters and near channel groundwater flow parallel to the river channel [e.g., (Woessner, 2000)] for extended distances (Hauer et al., 2016; Helton et al., 2014; Liang et al., 2018; Sawyer et al., 2009; Stanford & Ward, 1993; Ward & Stanford, 1993; Zachara et al., 2016). Hyporheic corridor flow is poorly documented and understood, yet it is an apparent common aspect of gravel-bed river corridors (Hauer et al., 2016; Valett et al., 2014).

Exchange flows vary with river size, type, channel geomorphology, subsurface hydrogeology, and flow conditions (Harvey, 2016; Harvey et al., 2018; Harvey & Gooseff, 2015; Helton et al., 2014; Poole, 2010; Poole et al., 2006; Valett et al., 2014). However, the extent and spatial variability of extended lateral hydrologic exchanges (e.g., >50 m) have been infrequently documented in larger river corridors (Covino, 2017). Limited study suggests that extended lateral hydrologic exchange can strongly influence the behavior of groundwater solute plumes in the river corridors (Mwakanyamale et al., 2012; Slater et al., 2010; Zachara et al., 2016; Zachara et al., 2013), but a generalized understanding of the interacting processes affecting the hydrogeochemistry of these systems does not exist (McCallum et al., 2010). Consequently, their impacts on the water quality of river corridor systems, and the features and processes governing them are not well understood.

Characterization of hydrologic exchange zones in large river systems is complicated by complex river channel structures and flood plain characteristics (Poole, 2010; Poole et al., 2004; Valett et al., 2014), inaccessible and heterogeneous subsurface geomorphic and hydrogeologic features (Amoros & Bornette, 2002; Heeren et al., 2014; Jones et al., 2008; Poole et al., 2006), and river discharge variations (Heeren et al., 2014; Siergieiev et al., 2015). Accordingly, the identification of hydrologic exchange zones along large river reaches are rare, but limited studies reveal high spatial variability (Johnson et al., 2015; Mwakanyamale et al., 2012; Slater et al., 2010) and poor predictability. Even fewer studies have considered and/or modeled solute transport or plume behavior during active, dynamic hydrologic exchange in larger river corridors (Jolly et al., 1998; McCallum et al., 2010). These gaps are made acute by the fact that large river corridors and their aquifers and hyporheic zones are heavily disturbed by widespread development and other exploitation (Tockner et al., 2008).

In this communication, we utilized a well-characterized field site containing a mobile groundwater uranium (U_{aq}) plume located within a major gravel-bed river corridor to investigate the dynamic pathways of hydrologic exchange flows. We developed a three-dimensional (3-D) groundwater flow and transport model to integrate and assess the influences of dynamic river stage variations and variable subsurface topography on hydrologic exchange and their consequent effects on flow, specific conductance (SpC), and U_{aq} concentrations within the river corridor. We explored the influences of: 1) river stage on hydrogeologic connectivity along the river bank, 2) hydrologic exchange between surface water and groundwater on hyporheic water composition, and 3) the structure of aquitard on water flow pathways through the plume and their attendant effects on SpC and U_{aq} concentrations. Our study suggests that dynamic hydro-geochemical behaviors observed in other gravel-bed systems be likewise interpreted within the context of hydrologic exchange.

2. Methods

2.1. Site Characteristics

Field research was performed in the Columbia River corridor at the Hanford 300 Area in south-central Washington State (Figure 1a). The 300 Area contains a persistent groundwater uranium plume resulting from historical nuclear fuel fabrication (Figure 1a), which has been the object of many previous studies [e.g., (Chen et al., 2013; Chen et al., 2012; Murray et al., 2013; Rockhold et al., 2013; Zachara et al., 2016; Zachara et al., 2013)]. The uranium plume is hosted in a shallow, unconfined flood plain aquifer with a seasonally-varying water table of 7-10 m below ground surface (Figure S1). The aquifer is comprised of unconsolidated, gravel-textured, Pleistocene-age flood deposits (Hanford formation), which overlie a Pliocene-age, basal aquitard/bedrock (Ringold Formation) comprised of semi-consolidated, fine-grained fluvial sediments. The surface of the basal aquitard for the flood plain aquifer

displays complex topography (90-105 m; Figure 1b) as a result of late Pleistocene erosional events that carved drainage channels in its surface (Figure S2). The thickness of the unconfined aquifer varies from <1 m in the north and east to ~17 m in the central and south quadrants (Figure 1b). Both the aquitard and the coarse-textured aquifer sediments outcrop along the river shoreline and the riverbed, covered by a thin veneer of recent alluvium.

The Columbia River at the field site occupies a channel with an approximate basal elevation of 90 m above sea level (MASL), with the river surface at ~104 m at low flow and ~107.5 m at high flow (Figure S1). Discharge ranges between 1900 and 5600 m^3/s depending on season. The water table elevation in the flood plain aquifer within 500 m of the river shoreline (104 - 107 m) responds rapidly to river stage changes that may exceed 3 m on a seasonal basis and ~1 m on daily and hourly basis from upstream hydropower generation [Figure S3a; (Zachara et al., 2016)]. These fluctuations create an extended para-fluvial zone most evident at low river flow (Figure S3b).

Locations of stage-driven hydrologic exchanges have been inferred along the river shoreline at the site from distributed temperature (Mwakanyamale et al., 2012; Slater et al., 2010) and electrical resistance tomography [ERT; (Johnson et al., 2012; Johnson et al., 2015; Wallin et al., 2013)] measurements. These locations (north and south channels; Figure 1b) appear to correlate with thicker, high-permeability deposits that fill the erosional channels. Groundwater and river water differ markedly in SpC (~450 µS/cm and ~120 µS/cm for groundwater and river water, respectively), which allows groundwater/river water mixing to be accurately determined by SpC measurements as shown in our previous study that explores the influence of seasonal river discharge variations and river water intrusion on U_{aq} and SpC dynamics (Zachara et al., 2016). Based on waters sampled during calendar years 2010-2012 from a compact, triangular, inland well-field (1800 m^2) near the center of the U_{aq} plume (Integrated Field Research Challenge (IFRC) site Figure 1b). Contemporaneous well-water

U_{aq} concentrations were observed to vary markedly between nearby wells as the water table rose and fell in response to river stage variations, with differences attributed to vertical and horizontal hot spots of residual, sorbed uranium in the vadose zone (Murray et al., 2013), groundwater flow direction reversals, and river water intrusion.

2.2. Groundwater Sampling and Analysis

In this study, we expand to a much larger area representative of the uranium plume as a whole, including observation points both near and far from the river shoreline with high-resolution temporal monitoring data from calendar years 2013-2015, to understand the influence of various hydrologic exchange pathways on fate and transport of contaminant plumes in the river corridor. We monitored 13 wells (see Table S1 and Figure 1b for detailed well locations) located over a range of distances from the river shoreline (50 to 500 m; circles in Figure 1b) for SpC and U_{aq}. Over 1147 individual well water samples were collected and analyzed on weekly to biweekly basis. All of the wells were instrumented with pressure transducers for constant monitoring of water level; a subset (2-01, 2-02, 1-21A, 3-19, 2-32, 2-33, 2-05, 1-10A) was also instrumented with sensors for SpC. River stage and SpC was constantly monitored at a river gauge (SWS-1) near the south channel (Figure 1b). Most of the wells were located within, or proximate to the north channel terminating in an identified exchange zone along the river shoreline (Figure 1b; wells 1-21A, 2-01, 2-02, 2-03, 2-05, 2-07, 2-23, 2-32, 2-33, 3-19), while three others (1-10A, 3-09, and 4-09) were located outside of this zone. Among those wells, 2-05, 2-07 and 2-23 were also included in the earlier study that focused on the uranium plume transport within the triangular IFRC site (Figure 1b). They are located further away from the shoreline.

The wells were sampled by bailing from an approximate depth of 0.25 m below the water table. Several bailers of water were retrieved and discarded to assure the upper stagnant water

had been removed. The well water is usually well-mixed due to high flow velocity at the site. The SpC, pH, and temperature of sampled well-water was measured at the time of collection. The SpC can be used as a conservative tracer since it is strongly correlated with chloride concentration with an R^2 of 0.83 (Figure S9). The water samples were then filtered (0.2 um Millipore IC Millex Teflon syringe filter #SLLGC25NS), and samples for U_{aq} analysis were preserved with 70% ultrapure, double distilled nitric acid. U_{aq} analyses were performed with a kinetic phosphorescence analyzer (KPA-11, Chemchek Instruments, Richland, WA). Calibration curves were made from certified single-cation ICP standards (UltraScientific, Kingston, RI) diluted over the appropriate analyte concentration range. Dilutions for U_{aq} analyses, when required, were performed with 70% ultrapure, double distilled nitric acid. Analytical uncertainty was <10%.

The well screen intervals vary as they were placed for different purposes (compliance monitoring or research). The compliance monitoring wells were screened over the entire thickness of the saturated zone, which commonly demonstrate intra-borehole vertical flows (can be up or down depending on river stage dynamics and consequent vertical gradients) (Vermeul et al., 2011). Borehole flow creates "noise" in the resulting data (Zachara et al., 2016) as analyte concentrations in the aquifer can vary vertically depending on the season and hydrologic condition. Research wells sampled the upper portion of the saturated zone (approximately 103-106 m) with a 3 m screened interval. The research wells displayed lesser, but still noticeable effects of intra-borehole flow.

2.3. Flow and Transport Model

A 3-D groundwater flow and transport model was implemented in PFLOTRAN (Hammond et al., 2014) that simulates variably saturated flow using Richard's Equation with a finite-volume approach. The modeling domain is 3300 m × 1900 m × 22 m (88-110 MASL)

(Figure 2), with the Columbia River bounding on the east side. The overall modeling domain were selected to be big enough to minimize the boundary effects on the simulated system responses in our monitoring domain (red box in Figure 2). Grid size was 4 m in the horizontal and 0.5 m in the vertical with a total of ~17 million cells.

Accurate subsurface topography for the basal aquitard and its exposure along the river shoreline (Figure 1b) was obtained from well logs. The aquifer contains three distinct geologic units, Hanford formation gravel, Ringold Formation fines, and Ringold Formation gravel (Williams et al., 2008). Although significant vertical and horizontal heterogeneity have been revealed in the Hanford formation gravel from extensive field characterization efforts (Chen et al., 2013), we assumed homogeneity with each formation to focus on assessing the influence of subsurface structure and river stage dynamics on hydrologic exchange flows. Porosity and hydraulic conductivity values for the Ringold and Hanford formation sediments were taken from a previous study (Chen et al., 2013). The Hydraulic conductivity of Hanford formation (~7000 m/d) is 2 to 3 orders of magnitude higher than that of the Ringold formation (1~40 m/d). The vertical to horizontal hydraulic conductivity ratio was set to 0.1. The molecular diffusion coefficient was set to 1×10^{-9} m^2/s. Although PFLOTRAN does not account for mechanical dispersion, its effects are negligible compared to macrodispersion caused by spatial heterogeneity in hydraulic conductivity as shown in our previous studies (Chen et al., 2012; Chen et al., 2013). Characterizing physical heterogeneity of the aquifer can further improve the representation of effective dispersion in our numerical model (see Discussion 4.1). Details of the hydraulic parameters provided in Table S2 in the Supporting information.

There is a long record of hydrologic monitoring data equating well-water levels to Columbia River elevation [(Chen et al., 2012; Hammond & Lichtner, 2010; Rockhold et al., 2013); see example data in Figure S3]. Thus, the spatial response of the water table to river

elevation changes can be reasonably described to the hour (Chen et al., 2013). Inland boundaries were applied using hydraulic head values kriged from hourly groundwater table elevations monitored in proximate wells. River surface elevations were prescribed along the river shoreline using simulation results of the river routing model MASS1 (Modular Aquatic Simulation System in 1-Dimension) (Niehus et al., 2014; Richmond, 2014), which has been applied to the Hanford reach based on channel physiographic and bathymetric measurements, and measured discharge from the upstream Priest Rapids Dam. Both of the simulated hourly river elevations and kriged inland groundwater table elevations were smoothed using a 6-hour moving average window to facilitate model convergence while preserving subdaily to daily fluctuations. Simulations were performed for calendar years 2010-2014 at a maximum time step of 6h, with the first three years considered as a spin-up period.

Hydrologic exchanges between flood-plain groundwater and the Columbia River is influenced by a layer of recent, poorly sorted alluvium that is overlain by coarse riverbed armor. As this alluvial layer has a lower hydraulic conductivity than coarse-textured Hanford formation sediments lying immediately below in the para-fluvial zone and the river channel, it dampens the effects of river stage fluctuations on groundwater table variations and hydrologic exchange (Hammond & Lichtner, 2010). Such damping effect was represented by a time-invariant conductance boundary condition at the sediment-river interface in our model, equivalent to adding a low-permeability layer with the thickness of half-cell length (about 2m horizontally and 0.25 m vertically in our case). An optimal set of conductance values (5.23×10^{-14}, 6.31×10^{-14}, 1.47×10^{-13}, and 1.60×10^{-12} m for upstream, north, middle, and south river segments, respectively) was selected from multiple realizations based on the fit between the simulated and observed hydraulic head and SpC in near-shore wells (details provided in Text S1 in the Supporting Information).

Non-reactive in-silico tracers were placed along the north inland boundary (GW tracer) and along four river shoreline segments (upstream, north, middle, and south, Figure 2) to assess predominant flow directions and velocities influenced by dynamic river elevation variations and the variable subsurface topography of the basal aquitard and its outcrop along the river. Normalized breakthrough concentrations (C/C_0) for tracers originating from the five different locations in the modeling domain were calculated at each observation well during the simulation period. The concentrations of individual river tracers and their sum were compared to measured, normalized values of SpC to ascertain potential water sources and flow paths for wells situated at different spatial locations in the plume at different distances from the river shoreline. They were also compared to well-water concentrations of U_{aq} to elucidate the influence of various exchange flow pathways on the contaminant transport and contributions of heterogeneous uranium sources.

3. Results

3.1. Temporal Trends in Observed Groundwater Concentrations

The maximum Columbia River water stage for the study period (4/2/13 – 2/28/15) reached ~107 m during the spring 2014 snowmelt (Figure S3a), well below the maximum elevations observed in 2011 and 2012 [>108 m; Zachara et al. (2016)]. However, the monitoring data revealed that the river stage fluctuations in 2013 and 2014 caused significant temporal variations in both U_{aq} concentration and SpC in all wells (Figure S4). Considering a subset of the wells (Figure 3), it was evident that the geochemical effect of hydrologic exchange flows varied with distance from the river (note differences in scale for the different panels). Generally, wells proximate to the river (~50 m inland) displayed low concentrations of U_{aq} and SpC during high spring river flows, and elevated concentrations during periods of low river flow, with inflections noted at times of rapid river elevation changes. In contrast,

the most inland wells (~500 m) displayed an inverse trend. Wells at intermediate distance (~250 m inland) displayed complex and intermediary behavior with: 1) fluctuating U_{aq} and SpC concentrations during the high flow periods, 2) initially high but decreasing U_{aq} concentrations during the period of river stage decrease, and 3) relatively constant, and high values of SpC for the entire period between river flow maxima.

SpC values below ~450 were indicative of the proportional mixing of river water with groundwater through hydrologic exchange. The near-shore wells (~50 m inland) displayed periods when their waters were dominated by either river water (June 2013 and June 2014) or groundwater (August 2013-March 2014). However, sustained periods of SpC between 350 and 400 µS/cm in 50 m inland wells 2-01 and 2-02 during September to the following March indicated a lingering river water influence during the low flow period. High-frequency, smaller SpC spikes during these periods were indicative of temporal advances and/or retreats of either river water or groundwater in response to high-frequency river stage oscillations resulting from upstream hydropower dam operations and attendant pressure changes along the river shoreline. The inland wells (~500 m) displayed no evidence for river water based on SpC, but elevated SpC (~500 µS/cm) above average groundwater values was observed at the highest river and groundwater table elevations (106-107 m). Dips in SpC at the intermediate distance wells (~250 m inland) during high river stages were indicative of inland migration of river water, approximately 50% to 40% of river water.

The relationships of SpC and U_{aq} to river stage, and hence groundwater table, were strongly influenced by the well distance from the river shoreline (shown for representative wells in Figure 4, others in Figure S5). The near-shore wells (e.g., 2-02, Figure 4a) displayed a strong negative correlation and a hysteresis loop between SpC and U_{aq} with groundwater table elevation as it rose above the baseline of 105 m, indicating progressive dilution of groundwater by river water as river stage increased. The hysteresis loop indicated different

contributing sources of SpC and U_{aq} during the rising and falling limbs of river stages. At intermediate distances (e.g., 250 m, well 2-32), the arrival of river water was noted by the decrease in well-water SpC beginning at a groundwater table of 106 m (Figure 4b). U_{aq}, in contrast, displayed little correlation with water table elevation at intermediate distance, although concentrations tended to decrease at the highest water table elevations (e.g., >106 m) with the arrival of river water. SpC at the most inland distance (500 m, wells 1-21A and 3-19) showed no evidence for the presence of river water, but increased mildly with the rising groundwater table (Figure 4c). U_{aq} concentrations tended to increase with groundwater table at this location but the overall correlation for the two-year period was poor. Overall, SpC appeared to conform to a mixing model at near-shore and intermediate distances with groundwater and river water endmembers, while U_{aq} did not. Highly correlated behavior between U_{aq} and SpC was only observed in the near shore (e.g., 2-01, 2-02, 1-10A, and 4-09) and inland (1-21A, 3-19) wells.

The adsorptive retardation of U_{aq} in the saturated zone has been shown to be small because of coarse sediment texture and a low concentration of surface complexation sites (Zachara et al., 2016). In spite of predominant hydrologic control, the trends in U_{aq} concentration in the different wells were more complicated to interpret than SpC as a result of multiple factors including: 1) spatially and temporally heterogeneous U_{aq} concentrations in the plume (Figure 1a), 2) U_{aq} solubilization from heterogeneously distributed source areas in the lower vadose zone (mostly within the intermediate distance from the river) during high water table periods (Murray et al., 2013; Zachara et al., 2016), and 3) multi-directional transport from source zones in different areas of the plume and intra-wellbore flows during rising and falling water tables.

3.2. Model Evaluation

Utilizing the high-performance computing, we were able to run a 5-year PFLOTRAN simulation with 2048 processor cores in less than 12 hours (computation/wallclock time). The model converged with minimal mass balance error. The normalized concentration of each of the tracers within each of the wells was calculated from the model output data for the two-year monitoring period. These values were compared to the normalized concentrations (NC) of SpC and the observed concentrations of U_{aq}. The NC of SpC was defined as $NC = (C_t - C_{min})/(C_{max} - C_{min})$ where C_t is the observed concentration at any point in time (t), and C_{max} and C_{min} are the maximum and minimum observed SpC in all wells over the monitoring period. The modeling results are discussed in context of our baseline conceptual model for the system: that the presence of river water (from either the upstream, north, middle, or south river tracers) causes a proportional decrease in groundwater SpC and U_{aq} by dilution. Observations consistent with this dilution model are termed “expected”, whereas those that are inconsistent are termed “unexpected”.

Given various assumptions in our hydrologic model including the homogeneity of hydraulic properties in each hydrogeological formations, the computed tracer breakthrough behavior suggested that at any given time, well waters were generally dominated by a single source originating from the model boundaries (e.g., groundwater or river; Figure 5). The timing of dominance for the different source terms varied temporally within a given year and were controlled by river stage and groundwater table. These patterns repeated themselves during the two-year monitoring period (2013 and 2014) because of the similarity in their annual hydrographs.

Shifts in water sources as implied by tracer concentrations were often associated with inflections in the monitoring data. For example, well 2-02 was dominated by the north and middle river tracers when SpC was low, and by groundwater when SpC was high (Figure 5a),

"expected" observations. SpC decreases were also noted in intermediate well 2-32 when the mass fraction of the middle river tracer was high (e.g. ~0.5; Figure 5b, "expected"), but not during the subsequent passage of the diluted north and upstream tracers ("unexpected"). Inland well 1-21A displayed an anomalous trend in observed SpC relative to the other wells, increasing by 20 % during periods of high river stage (Figure 5c). Model simulations implied the intrusion of upstream and north river tracers to well 1-21A at mass fractions of approximately 0.3 during high river stages (Figure 5c). This degree of river water intrusion was "unexpected" because the monitored SpC data showed no evidence for river water.

The observed U_{aq} concentrations also displayed fair agreement with the simulated presence of waters from different sources. River water associated with the north and middle tracers correlated with reduced U_{aq} concentrations in shoreline well 2-02 and intermediate well 2-32 (Figures 5a and 5b, "expected"), whereas upstream tracer waters did not ("unexpected). The upstream tracer was associated with an increase in U_{aq} in well 2-02, and a slowly decreasing concentration in well 2-32. Simulation results implied that the intrusion of river water from upstream and north tracer locations might explain the increases in U_{aq} concentration in well 1-21A during periods of high river stage (Figure 5c), suggesting that river water or rising groundwater following their flow paths may have been enriched in desorbed U_{aq} from the lower vadose zone. Indeed, waters of high U_{aq} concentration (>1000 µg/mL) were collected from the top of the water table in the northern section of the modeling domain in the spring of 2011 (unpublished data). SpC observations at this well displayed no evidence of river water presence, which indicated that the changes of SpC and U_{aq} in the inland well 1-21A were likely due to displacement of groundwater with varying geochemistry. While such displacement was driven by the intrusion of river water from the upstream and north river segments, the extent of their intrusion seemed to be over-estimated at this inland location by our model.

3.3. Simulated Exchange Flow Dynamics

Model simulation revealed complex and dynamic water flow paths and groundwater and river water mixing through the study domain as shown in Figure 6 at five different river stages covering both rising and falling limbs of the hydrograph, including antecedent low river stage (02-24-2014, Figure 6a), ascending river stage (04-25-2014, Figure 6b), river stage maximum (05-25-2014, Figure 6c), descending river stage (08-03-2014, Figure 6d), and post intrusion low water (09-22-2014, Figure 6e). Each of these figures presents separate panels for the groundwater flow vectors, plumes of groundwater tracer and river tracers for the noted dates. Velocity vectors at 104 m were selected to illustrate the flow dynamics, which showed similar patterns at other elevations. The groundwater tracer is shaded according to groundwater mass fraction (GMF) ranging from 1 (all groundwater, dark red) to 0 (all river water, white). The river tracers are shaded according to origin (upstream-purple, north-green, brown-middle, and south-cyan); areas shaded by these colors simply denote the presence of river water without regard to its mass fraction. At any specific location, total river tracer (TRT) = 1 – GMF.

At a low river stage (Figure 6a), groundwater flow was predominantly from the NW to SE, with discharge to the river occurring primarily through the south channel. Flow velocities were small (median value is 0.007 m/d) and consistent with the baseflow discharge condition to the river. At a high river stage (Figure 6c), river water intruded from the NE to SW into the near-shore aquifer that changed the direction of groundwater flow by approximately 90^{o} from during the low river stage. The resulting predominant subsurface flow vectors were from the east (the river) to the west (inland) with significant local variations in both direction and magnitude (median value is 0.008 m/d)). After passage of the high river stage period (Figure 6d), river water started to drain from the aquifer to the river, primarily through the paleo-

channel from north to southwest. The velocities at the falling limb (median value is 0.015 m/d) were significantly higher than those at rising and baseflow conditions. Subsurface flow velocities varied with aquitard topography and corresponding aquifer thickness, with higher velocities occurring in thinner, saturated zone domains. Velocity magnitudes also increased with depth (elevation 105 to 102 m; Figure S6) as aquitard high spots blocked flow, causing greater flux in the deeper erosional channels. Generally, the flow field changed rapidly at all dates with frequent ~1 m daily fluctuation in river stages (see Movie S1 in the supporting information for a subdomain of the model (Figure 1)), with significant influences of antecedent conditions (e.g., rising or falling water table). These dramatic changes in groundwater flow directions with river stage variations indicated that upgradient domains contributing to solutes in each of the wells changed as frequently in response to the river hydrograph.

The model domain was dominated by groundwater at antecedent low river stage (Figure 6a) after experiencing over three months of continuous low river stage (<105.5 m). A small amount of residual river water (e.g., upstream, north, middle, and south river tracers) from the previous year (spring 2013 intrusion event) remained in the middle and southeast quadrants of the domain along the shoreline proximate to wells 2-01 and 4-09 (~50% river water), consistent with monitoring data (Figure 3). River water concentration was highest near well 2-01 where the aquitard was at high elevation and the saturated zone was thin (Figure 1b).

River water intruded the site unevenly along the entire shoreline during ascending river stage (Figure 6b), resulted from the variable thickness of Hanford formation exposed to river water. Groundwater was displaced to the west, and near-shore wells (1-10A, 2-02, 2-03, 2-01, and 4-09) displayed high river water fraction (e.g., GMF<0.35). Intruded river water plumes from the upstream, north, middle, and south locations coalesced into a continuous domain of downriver hyporheic corridor flow roughly parallel to the shoreline. River water intrusion

continued to the highest river elevation (107 m on 05-25-2014, Figure 6c), expanding the zone of hyporheic corridor flow over that observed at ascending stage. A zone of high river water mass fraction developed in near-shore wells monitoring the north channel (2-01, 2-02, and 2-03). The development of hyporheic corridor flow in the flood plain aquifer during periods of high river stage was clearly demonstrated in the animations of these simulations (see Movie S2 in the supporting information).

The zone of river water influence expanded to its maximum inland extent at descending river elevation (Figure 6d), when all of the monitored wells except 1-21A and 3-19 displayed low GMF. Maximum inland river intrusion was delayed, relative to maximum river stage, by over one month. Inland river water penetration was greatest along the north channel axis. Drainage of hyporheic corridor flow through the south channel to the river was evident from the decreased footprint of the south tracer on 08-03-2014 (Figure 6d) as compared to 05-25-2014 (Figure 6c).

Displacement of river water from the monitoring domain by groundwater proceeded from north to south (Figure 6e). As the river elevation returned to pre-intrusion levels, waters with high river water mass fraction remained in the north channel, in the thin saturated zone near well 2-01, and in downstream well 4-09. Hyporheic corridor flow became discontinuous, occurring along the central and south shoreline. The amount of residual river water present in the domain at this date (09-22-2014) significantly exceeded antecedent (02-24-2014) levels, exhibiting residence times in excess of six months.

3.4. Impacts of Hydrogeological Structure and River Stage Dynamics on Hydrologic Exchange Flows

Our modeling results provided rich spatial and temporal information to understand the HEF dynamics and spatial patterns across the entire model domain, which are often difficult to derive from the point-based observations. Thus, we performed spatio-temporal clustering

analysis (details provided in Text S2 and Figure S8 in the Supporting Information) on 136 simulated total river tracer (TRT) snapshots (one every five days between March 2013 and December 2014) to evaluate the influences of hydrogeological structure and hydrological dynamics on exchange flows. Only the areas with more than 1% of TRT in aquifer were included in the clustering analysis (marked by the black spline line in Figure 7a).

We identified six distinct clusters as spatially mapped in Figure 7a, overlaying above the topography of the Hanford-Ringold interface. Spatial cluster 1 (brown) represents the most dynamic river tracer behaviors, as shown in the tracer time-series plots (brown, Figure 7b). Spatial cluster 1 is located close to model south and north boundaries yet outside of our monitoring domain (red dashed box), confirming that the boundary effects were not propagated to our main area of interest. Spatial cluster 6 (red) is the second most dynamic cluster located near the shoreline. Interestingly, spatial cluster 3 (blue) transverses the north entrance of deep erosional channel and connects to the river. Spatial cluster 4 (purple) covers the area in the southern part of the paleo-channel. Spatial cluster 2 (green) covers the transition between spatial cluster 3 and spatial cluster 4. Spatial cluster 5 (orange) occupies the upstream inland part of the river corridor, exhibiting fast intrusion and retreat of the river water, as controlled by the thinner Hanford formation. The clustering results clearly demonstrated the impact of subsurface hydrogeology on hydrological exchanges in a dynamic system.

We then applied the same clustering algorithm over the sampled SpC observations of the 13 wells and identified three major clusters as shown in Figure 7a (black scatters). Although the mapping of the well clusters does not exactly match the clustering mapping of the simulated TRT, we still observed general consistent spatial correspondence between the well clustering of observations and spatial clustering of simulations. For example, the inland well clusters 1 (points) and 2 (triangles) appeared in inland spatial clusters 2 (green) and 4

(purple), and the near-shore well cluster 3 (crosses) was related to near-shore spatial cluster 3 (blue) and 6 (red). The difference could be partially attributed to the variabilities in well screen depths and coarser temporal and spatial resolution of the sampling data, which could impact the boundary delineation between the clusters.

Three major temporal clusters were identified by analyzing all the snapshots of simulated TRT. As shown in Figure 8, the temporal clusters correspond well with three primary phases of river hydrograph, i.e., high, rising from low to high, and falling from high to low. The temporal cluster 1 (blue) corresponds to the periods of high river stage, exhibiting the largest river intrusion in the aquifer (left subplot in Figure 8b). The temporal cluster 2 (red) occurred during periods of low and initial ascending river stage with minimum mean river tracer concentrations (middle subplot in Figure 8b). The temporal cluster 3 (green) represents the periods of descending river stage periods (right subplot in Figure 8b), featuring river water retreat through the paleo-channel to the south.

4. Discussion

4.1. Conceptual model uncertainty and limitations

Our assumption of within-formation homogeneity in hydraulic properties represents a source of uncertainty by ignoring locally expedited or retarded movement of water. Significant physical heterogeneity at the local scale (5-25 m) has been revealed by geophysical measurements and tracer experiments in the central part of our modeling domain. Flow and transport in the Columbia River corridor is influenced by heterogeneous distribution of highly permeable clast-supported gravels and less permeable lenses of silty sand (Chen et al., 2013; Chen et al., 2012). Unfortunately, similar level of characterization effort was not available for the large portion of the current modeling domain. Studies in other gravel-bed river corridors have also revealed the presence of localized, geomorphologically-controlled preferential pathways such as buried paleochannels that facilitate river water

migration to inland, subsurface locations (Brunke & Gonser, 1997; Malard et al., 2002; Sophocleous, 2002; Stanford et al., 2005). Our model evaluation has shown that characterizing the physical heterogeneity in the Hanford formation and riverbed alluvial layer could have improved the ability of our numerical model to reproduce the observed behaviors. However, such efforts are highly challenging in terms of both computational and experimental or monitoring costs. More research is desired to seek affordable aquifer characterization strategies for kilometer-scale systems and beyond.

4.2. The Importance of Scale-dependent Hydrologic Exchange Flows

Our results demonstrated the importance of studying extended hydrologic exchange flows over a large range of temporal and spatial scales. Compared to a previous study by Zachara et al (2016), this study encompassed a much larger area with extended lateral flow-paths through the river bank and associated river corridor aquifers. We showed that the groundwater-surface water interaction zone extended normal to the river axis for approximately 400-500 meters, and parallel to the axis for distances in excess of 1.5 km, which could not be captured by our previous study (Zachara et al., 2016). River stage variations were especially important for the gravel-bed river corridor studied here, creating a nested pattern of hydrologic exchanges ranging in time frame and excursion distance (Figure 9). Small 0.5 -1 m stage fluctuations occurring over hours to days created meter-scale hydrologic exchanges into the river bank of short residence time (Song et al., 2018), whereas seasonal 2-3.5 m stage fluctuations occurring over multiple month time periods caused extended, km-scale subsurface river water excursions with residence times in excess of 6 months. Once initiated by seasonal high-water events, extended inland excursions of river water continued unaffected by shorter-term, cotemporaneous meter-scale hydrologic exchanges driven by daily stage fluctuations. Similar hierarchical hydrologic exchange

behaviors have been proposed but rarely documented in other large riverine systems (Covino, 2017; Poole, 2010).

Hyporheic corridor flow reached its maximum lateral and inland extent approximately two months after peak river stage (Figure 6d); the delay being a product of sediment hydraulic conductivity, boundary conductance, and groundwater and river water head/pressure gradients. Hyporheic corridor flow decreased thereafter for 6 months (see Movie S2). Significant river water (30-70%) remained in the near-shore region of the exchange zone for over 1 year following the previous year's high stage event (Figure 6a), apparently promoted by flow blockage caused by uneven aquitard topography. These long residence times (from 6 months to over 1 year) may be representative of other large, gravel-bed river corridors where skeletal sediments and high subsurface permeability permits extended inland excursions of river water. While any field site chosen for study may exhibit unique properties and characteristics that challenge applicability of results elsewhere, this particular reach of Columbia River displays hydro-geophysical attributes that are common to other managed gravel-bed riverine systems, world-wide, that are important for water supply and fisheries [e.g., (Church et al., 2012; Hauer et al., 2016; Heeren et al., 2011; Jones et al., 2008; Malard et al., 2002; Malcolm et al., 2003; Mejia et al., 2016; Vervier et al., 2009; Wilcock et al., 1996)]. Similar km-scale field and modeling studies are particularly suited to develop fundamental understanding of spatial and temporal patterns of hydrologic exchanges across the range of scales because it is large enough to capture larger-scale exchanges such as the hyporheic corridor flow yet it is still affordable to perform numerical simulations at the m-scale resolution.

4.3. The Effect of Hydrogeomorphic Template

The effects of discharge were superimposed on a hydrogeomorphic template (Covino, 2017; Poole, 2010) that controlled the locations, hydrologic connectivity, and overall

behavior of hydrologic exchange zones along the river corridor. The template is a combination of local geologic, hydromorphic, and geomorphic features that promotes hydrologic connectivity between the river channel and associated hyporheic waters under certain hydrologic conditions (Poole, 2010). The hydrogeomorphic template for the Columbia River corridor involves the river channel exposure of highly permeable, flood deposited aquifer sediments, and the underlying topography of the less permeable aquitard surface (Figure S1). Complex, relatively impermeable subsurface bedrock structures block river water intrusion at certain locations, depths, and river stages; but facilitate it at others thereby defining a physical model for hydrologic exchange at the river corridor scale.

Our simulated hydrologic exchanges revealed strong correlation between the river tracer plume and the underlying hydrogeomorphic template through the clustering analysis shown in Section 3.4. Such correlations were also discovered through field monitoring of exchanges along the shoreline of our modeling domain using continuous waterborne electrical imaging (CWRI), fiber optic distributed temperature sensor (FO-DTS) monitoring (Slater et al., 2010) and time-lapse electrical resistance tomography (ERT) (Johnson et al., 2015). CWRI measurements indicated that the exchange zones occurred where highly permeable Hanford formation sediments were exposed at and below the river surface elevation (Figure S1), roughly correlating with low topographic domains of the basal aquitard surface (Figure 1b). During periods of low river stage, FO-DTS identified five groundwater discharge zones along the shoreline (~50-150 m in length), where riverbed water temperature anomalies were highly correlated with river stage (warmer and cooler anomalies during low stage in winter and summer, respectively).

ERT monitoring during periods of high river stage (from April 1, 2013 to November 4, 2013) illustrated that river water intrusion occurred unevenly along the entire river shoreline, with top-over of river water occurring above impermeable bedrock (Figure S7), which is

similar to the modeled behaviors shown in Figure 6. Also similarly, ERT monitoring identified the greatest river water fractions and the extent of inland penetration at high river stage in the north channel proximate to wells 2-02, 2-03, and 2-01. Furthermore, the ERT-measured pattern of lateral river water intrusion contains finer spatial structure and variations as expected from natural physical heterogeneities in both the unconsolidated alluvium and the aquitard surface that are known to exist at this location, but not accounted for in our model as discussed earlier.

4.4. Impacts of Hydrologic Exchange on Contaminant and Solute Transport in River Corridors

Uranium plume studied herein resides in a location of the river corridor with geomorphic characteristics that promote hydrologic exchange under conditions of both low and high discharge. Similar hydrologic exchange behavior appears to occur at other locations in the Columbia River corridor that exhibit comparable geomorphic and geologic characteristics. Variations in the physical template along the shoreline and in associated subsurface sediments lead to an apparent patchwork distribution of macroscopic exchange zones that vary in the detail of their hydrologic exchange behavior (Shuai et al., 2019). Two other well-studied Cr groundwater plumes (100 D and 100 H) exist in the river corridor some 35 km upstream of our study site that discharge to sensitive salmon spawning areas (PNNL, 1999). The two sites contain hundreds of monitoring locations (DOE, 2014, 2016, 2017) and two distinct plumes that have merged as a consequence of over 5 km of hyporheic corridor flow parallel to the river axis (Smoot et al., 2011). Like the U_{aq} plume studied herein, the Cr groundwater plumes display significant changes in concentration, SpC, and spatial extent and outline with large seasonal changes in river elevation (DOE, 2017). Near-shore monitoring wells have defined plumes of low SpC river water that intrude inland for ~200 m during

periods high river stage (DOE, 2016, 2017), and other locations of preferential discharge of high SpC groundwater containing Cr to the riverbed during low river stage.

It is exemplary of the types of dynamic behaviors that may be expected of poorly retarded contaminant plumes in other gravel-bed river corridors. At low stage, hydrologic exchange with meter-scale excursion distances promoted by hourly/daily river discharge variations caused significant short-term concentration variations in near-shore wells only. Periods of sustained high discharge promoted km-scale excursions of river water that moved far inland with long residence times. These large-scale excursions flooded near-shore wells with river water for month-long periods; displaced the contaminant plume inland with large attendant changes in groundwater flow direction, contaminant concentration, and plume outline; elevated the water table solubilizing lower vadose zone contaminants; and blocked plume discharge to the river, lengthening plume persistence.

5. Conclusions and Future Needs

In our study, we employed both field monitoring and numerical models to investigate the impacts of river discharge variations and subsurface hydrogeologic structure on kilometer-scale hydrologic exchange flows in the flood-plain aquifer of a major gravel-bed river system. We found that SpC and U_{aq} were strongly impacted by river intrusions in the near-shore wells. A strong negative correlation and a hysteresis loop existed between SpC and U_{aq} with groundwater table elevation. River stage variations superimposed on heterogeneous hydrogeomorphic template created a nested pattern of hydrologic exchanges ranging in various temporal and spatial scales, which are often difficult to derive from the point-based observations yet have important implications on contaminant plume migration.

The Columbia River corridor displays coarse-textured sediments and large seasonal stage fluctuations. It is expected that similar hydrologic exchange processes, varying with system

scale, hydrogeologic properties, and climate, occur in other gravel-bed stream and river systems, and their associated drainage corridors. The occurrence of potentially extended zones of hydrologic exchange should be considered when seeking to understand the biogeochemistry, elemental and heat budgets, and river corridor plume behavior of any riverine system susceptible to bank storage, lateral hydrologic exchange, and large stage fluctuations.

This study was made possible by: 1) large, spatially extensive, multi-modal data sets collected at a long-established field site, and 2) continuous monitoring of hydrologic exchange at selected locations using CWRI, FO-DTS, and ERT. Data sets of comparable density are economically impractical for most other large river corridors, especially for longer river reaches. A crucial scientific need is the documentation of new and/or improved methods (beyond those described herein) to identify locations of hydrologic exchange, the spatial areas of connected inland domains, and the magnitude of fluxes to and from extended subsurface zones accessible to both river water and groundwater. Mechanistic numerical modeling provides a robust way to advance our understanding of the spatial and temporal dynamics in complex system responses. It can form a solid basis for designing monitoring and experiments to assist decision making. The recent study of Shuai et al. (2019) serves as one example of such emerging approaches.

Acknowledgements

The research described in this publication was supported by the U. S. Department of Energy (USDOE), Biological and Environmental Research Division (BER), as part of BER's Subsurface Biogeochemical Research Program (SBR). Groundwater sampling and analysis was performed by Dr. Jim McKinley and Tom Resch as part of the monitoring program of the Hanford Integrated Field Research Challenge Project (IFRC). Statistical analyses,

groundwater flow modeling, and manuscript preparation were supported by the Pacific Northwest National Laboratory (PNNL), Subsurface Biogeochemical Research (SBR), Scientific Focus Area (SFA). PNNL is operated for the DOE by Battelle. All data described in this paper including modeling results can be found at: https://sbrsfa.velo.pnnl.gov/datasets/?UUID=ece70fb5-fc28-4f4b-b179-313b903d14aa.

Supporting Information

Additional supporting information may be found online in the Supporting Information section at the end of the article.

References

Amoros, C., & Bornette, G. (2002). Connectivity and biocomplexity in waterbodies of riverine floodplains. *Freshwater Biology, 47*(4), 761-776. doi:10.1046/j.1365-2427.2002.00905.x

Boano, F., Harvey, J. W., Marion, A., Packman, A. I., Revelli, R., Ridolfi, L., & Worman, A. (2014). Hyporheic flow and transport processes: Mechanisms, models, and biogeochemical implications. *Reviews of Geophysics, 52*(4), 603-679. doi:10.1002/2012rg000417

Boulton, A. J., Datry, T., Kasahara, T., Mutz, M., & Stanford, J. A. (2010). Ecology and management of the hyporheic zone: Stream-groundwater interactions of running waters and their floodplains. *Journal of the North American Benthological Society, 29*(1), 26-40. doi:10.1899/08-017.1

Bratley, P., & Fox, B. L. (1988). ALGORITHM 659: Implementing Sobol's quasi random sequence generator. *ACM Transactions on Mathematical Software, 14*(1), 88-100. doi:10.1145/42288.214372

Brunke, M., & Gonser, T. (1997). The ecological significance of exchange processes between rivers and groundwater. *Freshwater Biology, 37*(1), 1-33. doi:10.1046/j.1365-2427.1997.00143.x

Buffington, J. M., & Tonina, D. (2009). Hyporheic exchange in mountain rivers II: Effects of channel morphology on mechanics, scales, and rates of exchange. *Geography Compass, 3*(3), 1038-1062. doi:10.1111/j.1749-8198.2009.00225.x

Cardenas, M. B., & Wilson, J. L. (2007). Dunes, turbulent eddies, and interfacial exchange with permeable sediments. *Water Resources Research, 43*(8), W08412. doi:10.1029/2006wr005787

Chen, X., & Chen, X. H. (2003). Stream water infiltration, bank storage, and storage zone changes due to stream-stage fluctuations. *Journal of Hydrology, 280*(1-4), 246-264. doi:10.1016/S0022-1694(03)00232-4

Chen, X. Y., Hammond, G. E., Murray, C. J., Rockhold, M. L., Vermeul, V. R., & Zachara, J. M. (2013). Application of ensemble-based data assimilation techniques for aquifer characterization using tracer data at Hanford 300 area. *Water Resources Research, 49*(10), 7064-7076. doi:10.1002/2012WR013285

Chen, X. Y., Murakami, H., Hahn, M. S., Hammond, G. E., Rockhold, M. L., Zachara, J. M., & Rubin, Y. (2012). Three-dimensional Bayesian geostatistical aquifer characterization at the Hanford 300 Area using tracer test data. *Water Resources Research, 48*, W06501. doi:10.1029/2011wr010675

Church, M., Biron, P. M., & Roy, A. G. (2012). *Gravel-bed Rivers: Processes, Tools, Environments* (First ed.): John Wiley and Sons.

Covino, T. (2017). Hydrologic connectivity as a framework for understanding biogeochemical flux through watersheds and along fluvial networks. *Geomorphology, 277*, 133-144. doi:10.1016/j.geomorph.2016.09.030

Datry, T., Scarsbrook, M., Larned, S., & Fenwick, G. (2008). Lateral and longitudinal patterns within the stygoscape of an alluvial river corridor. *Fundamental and Applied Limnology, 171*(4), 335-347. doi:10.1127/1863-9135/2008/0171-0335

Dent, C. L., Grimm, N. B., & Fisher, S. G. (2001). Multiscale effects of surface-subsurface exchange on stream water nutrient concentrations. *Journal of the North American Benthological Society, 20*(2), 162-181. doi:10.2307/1468313

DOE. (2014). *Hanford Site Groundwater Monitoring Report for 2013* (DOE/RL-2014-32). Retrieved from U.S. Department of Energy, Richland Operations Office, Richland, WA:

DOE. (2016). *Calendar Year 2015 Annual Summary Report for the 100-HR-3 and 100-KR-4 Pump and Treat Operations, and 100-NR-2 Groundwater Remediation* (DOE/RL-2016-19, Rev. 0). Retrieved from U.S. Department of Energy, Richland Operations Office, Richland, WA:

DOE. (2017). *Hanford Site Groundwater Monitoring Report for 2016* (DOE/RL-2016-67). Retrieved from U.S. Department of Energy, Richland Operations Office, Richland, WA:

Dwivedi, D., Steefel, C. I., Arora, B., Newcomer, M., Moulton, J. D., Dafflon, B., . . . Williams, K. H. (2018). Geochemical exports to river from the intrameander hyporheic zone under transient hydrologic conditions: East River Mountainous Watershed, Colorado. *Water Resources Research, 54*(10), 8456-8477. doi:10.1029/2018wr023377

Gerecht, K. E., Cardenas, M. B., Guswa, A. J., Sawyer, A. H., Nowinski, J. D., & Swanson, T. E. (2011). Dynamics of hyporheic flow and heat transport across a bed-to-bank continuum in a large regulated river. *Water Resources Research, 47*, W03524. doi:10.1029/2010wr009794

Gu, C. H., Anderson, W., & Maggi, F. (2012). Riparian biogeochemical hot moments induced by stream fluctuations. *Water Resources Research, 48*, W09546. doi:10.1029/2011wr011720

Gupta, H. V., Kling, H., Yilmaz, K. K., & Martinez, G. F. (2009). Decomposition of the mean squared error and NSE performance criteria: Implications for improving hydrological modelling. *Journal of Hydrology, 377*(1-2), 80-91. doi:10.1016/j.jhydrol.2009.08.003

Hammond, G. E., & Lichtner, P. C. (2010). Field-scale model for the natural attenuation of uranium at the Hanford 300 Area using high-performance computing. *Water Resources Research, 46*(9), W09527. doi:10.1029/2009WR008819

Hammond, G. E., Lichtner, P. C., & Mills, R. T. (2014). Evaluating the performance of parallel subsurface simulators: An illustrative example with PFLOTRAN. *Water Resources Research, 50*(1), 208-228. doi:10.1002/2012WR013483

Harvey, J. W. (2016). Chapter 1 - Hydrologic exchange flows and their ecological consequences in river corridors. In E. H. Stanley & J. B. Jones (Eds.), *Stream Ecosystems in a Changing Environment* (pp. 1-83). Boston: Academic Press.

Harvey, J. W., Gomez-Velez, J., Schmadel, N., Scott, D., Boyer, E., Alexander, R., . . . Choi, J. (2018). How hydrologic connectivity regulates water quality in river corridors. *JAWRA Journal of the American Water Resources Association*, In press. doi:10.1111/1752-1688.12691

Harvey, J. W., & Gooseff, M. (2015). River corridor science: Hydrologic exchange and ecological consequences from bedforms to basins. *Water Resources Research, 51*(9), 6893-6922. doi:10.1002/2015wr017617

Hauer, F. R., Locke, H., Dreitz, V. J., Hebblewhite, M., Lowe, W. H., Muhlfeld, C. C., . . . Rood, S. B. (2016). Gravel-bed river floodplains are the ecological nexus of glaciated mountain landscapes. *Science Advances, 2*(6), e1600026. doi:10.1126/sciadv.1600026

Heeren, D. M., Fox, G. A., Fox, A. K., Storm, D. E., Miller, R. B., & Mittelstet, A. R. (2014). Divergence and flow direction as indicators of subsurface heterogeneity and stage-dependent storage in alluvial floodplains. *Hydrological Processes, 28*(3), 1307-1317. doi:10.1002/hyp.9674

Heeren, D. M., Fox, G. A., Miller, R. B., Storm, D. E., Fox, A. K., Penn, C. J., . . . Mittelstet, A. R. (2011). Stage-dependent transient storage of phosphorus in alluvial floodplains. *Hydrological Processes, 25*(20), 3230-3243. doi:10.1002/hyp.8054

Helton, A. M., Poole, G. C., Payn, R. A., Izurieta, C., & Stanford, J. A. (2012). Scaling flow path processes to fluvial landscapes: An integrated field and model assessment of temperature and dissolved oxygen dynamics in a river-floodplain-aquifer system. *Journal of Geophysical Research-Biogeosciences, 117,* G00n14. doi:10.1029/2012jg002025

Helton, A. M., Poole, G. C., Payn, R. A., Izurieta, C., & Stanford, J. A. (2014). Relative influences of the river channel, floodplain surface, and alluvial aquifer on simulated hydrologic residence time in a montane river floodplain. *Geomorphology, 205,* 17-26. doi:10.1016/j.geomorph.2012.01.004

Johnson, T. C., Slater, L. D., Ntarlagiannis, D., Day-Lewis, F. D., & Elwaseif, M. (2012). Monitoring groundwater-surface water interaction using time-series and time-frequency analysis of transient three-dimensional electrical resistivity changes. *Water Resources Research, 48,* W07506. doi:10.1029/2012wr011893

Johnson, T. C., Versteeg, R. J., Thomle, J., Hammond, G. E., Chen, X., & Zachara, J. (2015). Four-dimensional electrical conductivity monitoring of stage-driven river water intrusion: Accounting for water table effects using a transient mesh boundary and conditional inversion constraints. *Water Resources Research, 51*(8), 1-20. doi:10.1002/2014WR016129

Jolly, I. D., Narayan, K. A., Armstrong, D., & Walker, G. R. (1998). The impact of flooding on modelling salt transport processes to streams. *Environmental Modelling & Software, 13*(1), 87-104. doi:10.1016/S1364-8152(98)00003-6

Jones, K. L., Poole, G. C., Woessner, W. W., Vitale, M. V., Boer, B. R., O'Daniel, S. J., . . . Geffen, B. A. (2008). Geomorphology, hydrology, and aquatic vegetation drive seasonal hyporheic flow patterns across a gravel-dominated floodplain. *Hydrological Processes, 22*(13), 2105-2113. doi:10.1002/hyp.6810

Kalbus, E., Schmidt, C., Molson, J. W., Reinstorf, F., & Schirmer, M. (2009). Influence of aquifer and streambed heterogeneity on the distribution of groundwater discharge. *Hydrology and Earth System Sciences, 13*(1), 69-77. doi:10.5194/hess-13-69-2009

Kling, H., Fuchs, M., & Paulin, M. (2012). Runoff conditions in the upper Danube basin under an ensemble of climate change scenarios. *Journal of Hydrology, 424*, 264-277. doi:10.1016/j.jhydrol.2012.01.011

Li, H. L., Boufadel, M. C., & Weaver, J. W. (2008). Quantifying bank storage of variably saturated aquifers. *Ground Water, 46*(6), 841-850. doi:10.1111/j.1745-6584.2008.00475.x

Liang, X., Zhan, H., & Schilling, K. (2018). Spatiotemporal responses of groundwater flow and aquifer-river exchanges to flood events. *Water Resources Research, 54*(3), 1513-1532. doi:10.1002/2017wr022046

Malard, F., Tockner, K., Dole-Olivier, M. J., & Ward, J. V. (2002). A landscape perspective of surface-subsurface hydrological exchanges in river corridors. *Freshwater Biology, 47*(4), 621-640. doi:10.1046/j.1365-2427.2002.00906.x

Malcolm, I. A., Soulsby, C., Youngson, A. F., & Petry, J. (2003). Heterogeneity in ground water-surface water interactions in the hyporheic zone of a salmonid spawning stream. *Hydrological Processes, 17*(3), 601-617. doi:10.1002/hyp.1156

McCallum, J. L., Cook, P. G., Brunner, P., & Berhane, D. (2010). Solute dynamics during bank storage flows and implications for chemical base flow separation. *Water Resources Research, 46*, W07541. doi:10.1029/2009wr008539

McClain, M. E., Boyer, E. W., Dent, C. L., Gergel, S. E., Grimm, N. B., Groffman, P. M., . . . Pinay, G. (2003). Biogeochemical hot spots and hot moments at the interface of terrestrial and aquatic ecosystems. *Ecosystems, 6*(4), 301-312. doi:10.1007/s10021-003-0161-9

Mejia, F. H., Baxter, C. V., Berntsen, E. K., & Fremier, A. K. (2016). Linking groundwater - surface water exchange to food production and salmonid growth. *Canadian Journal of Fisheries and Aquatic Sciences, 73*(11), 1650-1660. doi:10.1139/cjfas-2015-0535

Meshkova, L. V., Carling, P. A., & Buffin-Belanger, T. (2012). Nomenclature, complexity, semi-alluvial channels, and sediment-flux driven bedrock erosion. In M. Church, P. M. Biron, & A. G. Roy (Eds.), *Gravel-Bed Rivers: Processes, Tools, Environments* (pp. 424-431). John Wiley and Sons.

Morrice, J. A., Valett, H. M., Dahm, C. N., & Campana, M. E. (1997). Alluvial characteristics, groundwater-surface water exchange and hydrological retention in headwater streams. *Hydrological Processes, 11*(3), 253-267. doi:10.1002/(Sici)1099-1085(19970315)11:3<253::Aid-Hyp439>3.0.Co;2-J

Murray, C. J., Zachara, J. M., McKinley, J. P., Ward, A., Bott, Y. J., Draper, K., & Moore, D. (2013). Establishing a geochemical heterogeneity model for a contaminated vadose zone - aquifer system. *Journal of Contaminant Hydrology, 153*, 122-140. doi:10.1016/j.jconhyd.2012.02.003

Mwakanyamale, K., Slater, L., Day-Lewis, F., Elwaseif, M., & Johnson, C. (2012). Spatially variable stage-driven groundwater-surface water interaction inferred from time-frequency analysis of distributed temperature sensing data. *Geophysical Research Letters, 39*, L06401. doi:10.1029/2011gl050824

Niehus, S. E., Perkins, W. A., & Richmond, M. C. (2014). *Simulation of Columbia River Hydrodynamics and Water Temperature from 1917 through 2011 in the Hanford*

Reach (PNWD-3278). Retrieved from Pacific Northwest National Laboratory, Richland WA:

PNNL. (1999). *Hanford Site Groundwater Monitoring for Fiscal Year 1998* (PNNL-12086). Retrieved from Pacific Northwest National Laboratory, Richland, WA:

Poole, G. C. (2010). Stream hydrogeomorphology as a physical science basis for advances in stream ecology. *Journal of the North American Benthological Society, 29*(1), 12-25. doi:10.1899/08-070.1

Poole, G. C., Stanford, J. A., Running, S. W., & Frissell, C. A. (2006). Multiscale geomorphic drivers of groundwater flow paths: subsurface hydrologic dynamics and hyporheic habitat diversity. *Journal of the North American Benthological Society, 25*(2), 288-303. doi:10.1899/0887-3593(2006)25[288:Mgdogf]2.0.Co;2

Poole, G. C., Stanford, J. A., Running, S. W., Frissell, C. A., Woessner, W. W., & Ellis, B. K. (2004). A patch hierarchy approach to modeling surface and subsurface hydrology in complex flood-plain environments. *Earth Surface Processes and Landforms, 29*(10), 1259-1274. doi:10.1002/esp.1091

Richmond, M. C. (2014). *Simulation of Columbia River Hydrodynamics and Water Temperature from 1917 through 2011 in the Hanford Reach* (PNWD-3278). Retrieved from Pacific Northwest National Laboratory, Richland, WA:

Rockhold, M., Bacon, D. H., Freedman, V. L., Parker, K. R., Waichler, S. W., & Williams, M. D. (2013). *System-Scale Model of Aquifer, Vadose Zone, and River Interactions for the Hanford 300 Area - Application to Uranium Reactive Transport* (PNNL-22886, RPT-DVZ-AFRI-019). Retrieved from Pacific Northwest National Laboratory, Richland, WA:

Rosenberry, D. O., Sheibley, R. W., Cox, S. E., Simonds, F. W., & Naftz, D. L. (2013). Temporal variability of exchange between groundwater and surface water based on

high- frequency direct measurements of seepage at the sediment- water interface. *Water Resources Research, 49*(5), 2975-2986. doi:10.1002/wrcr.20198

Sawyer, A. H., Cardenas, M. B., Bomar, A., & Mackey, M. (2009). Impact of dam operations on hyporheic exchange in the riparian zone of a regulated river. *Hydrological Processes, 23*(15), 2129-2137. doi:10.1002/hyp.7324

Shuai, P., Cardenas, M. B., Knappett, P. S. K., Bennett, P. C., & Neilson, B. T. (2017). Denitrification in the banks of fluctuating rivers: The effects of river stage amplitude, sediment hydraulic conductivity and dispersivity, and ambient groundwater flow. *Water Resources Research, 53*(9), 7951-7967. doi:10.1002/2017wr020610

Shuai, P., Chen, X., Song, X., Hammond, G., Zachara, J., Royer, P., . . . Huang, E. Y. (2019). Dam operations and subsurface hydrogeology control dynamics of hydrologic exchange flows in a regulated river reach. *Water Resources Research*, Accepted; WRCR23840. doi:10.1029/2018WR024193

Siergieiev, D., Ehlert, L., Reimann, T., Lundberg, A., & Liedl, R. (2015). Modelling hyporheic processes for regulated rivers under transient hydrological and hydrogeological conditions. *Hydrology and Earth System Sciences, 19*(1), 329-340. doi:10.5194/hess-19-329-2015

Slater, L. D., Ntarlagiannis, D., Day-Lewis, F. D., Mwakanyamale, K., Versteeg, R. J., Ward, A., . . . Lane, J. W. (2010). Use of electrical imaging and distributed temperature sensing methods to characterize surface water-groundwater exchange regulating uranium transport at the Hanford 300 Area, Washington. *Water Resources Research, 46*, W10533. doi:10.1029/2010wr009110

Smoot, J. L., Biebesheimer, F. H., Eluskie, J. A., Spiliotopoulos, A., Tonkin, M. J., & Simpkin, T. (2011). *Groundwater Remediation at the 100-HR-3 Operable Unit,*

Hanford Site, Washington, USA - 11507 (CHPRC-01149-FP). Retrieved from U.S. Department of Energy, Richland Operations Office, Richland, WA:

Song, X. H., Chen, X. Y., Stegen, J., Hammond, G., Song, H. S., Dai, H., . . . Zachara, J. M. (2018). Drought conditions maximize the impact of high-frequency flow variations on thermal regimes and biogeochemical function in the hyporheic zone. *Water Resources Research, 54*(10), 7361-7382. doi:10.1029/2018wr022586

Sophocleous, M. (2002). Interactions between groundwater and surface water: The state of the science. *Hydrogeology Journal, 10*(1), 52-67. doi:10.1007/s10040-001-0170-8

Stanford, J. A., Lorang, M. S., & Hauer, F. R. (2005). The shifting habitat mosaic of river ecosystems. *Verhandlungen des Internationalen Verein Limnologie, 29*, 123-136. doi:10.1080/03680770.2005.11901979

Stanford, J. A., & Ward, J. V. (1993). An ecosystem perspective of alluvial rivers - connectivity and the hyporheic corridor. *Journal of the North American Benthological Society, 12*(1), 48-60. doi:10.2307/1467685

Stonedahl, S. H., Harvey, J. W., & Packman, A. I. (2013). Interactions between hyporheic flow produced by stream meanders, bars, and dunes. *Water Resources Research, 49*(9), 5450-5461. doi:10.1002/wrcr.20400

Storey, R. G., Howard, K. W. F., & Williams, D. D. (2003). Factors controlling riffle-scale hyporheic exchange flows and their seasonal changes in a gaining stream: A three-dimensional groundwater flow model. *Water Resources Research, 39*(2), 1034. doi:10.1029/2002wr001367

Tockner, K., Bunn, S., Gordon, C., Naiman, R., Quinn, G., & Stanford, J. A. (2008). Flood plains: Critically threatened ecosystems. In N. Polunin (Ed.), *Aquatic Ecosystems: Trends and Global Prospects* (pp. 45-61). Cambridge University Press, Cambridge, UK.

Unland, N. P., Cartwright, I., Cendon, D. I., & Chisari, R. (2014). Residence times and mixing of water in river banks: implications for recharge and groundwater-surface water exchange. *Hydrology and Earth System Sciences, 18*(12), 5109-5124. doi:10.5194/hess-18-5109-2014

Unland, N. P., Cartwright, I., Daly, E., Gilfedder, B. S., & Atkinson, A. P. (2015). Dynamic river-groundwater exchange in the presence of a saline, semi-confined aquifer. *Hydrological Processes, 29*(23), 4817-4829. doi:10.1002/hyp.10525

Valett, H. M., Hauer, F. R., & Stanford, J. A. (2014). Landscape influences on ecosystem function: Local and routing control of oxygen dynamics in a floodplain aquifer. *Ecosystems, 17*(2), 195-211. doi:10.1007/s10021-013-9717-5

Vermeul, V. R., McKinley, J. P., Newcomer, D. R., Mackley, R. D., & Zachara, J. M. (2011). River-induced flow dynamics in long-screen wells and impact on aqueous samples. *Ground Water, 49*(4), 515-524. doi:10.1111/j.1745-6584.2010.00769.x

Vervier, P., Bonvallet-Garay, S., Sauvage, S., Valett, H. M., & Sanchez-Perez, J. M. (2009). Influence of the hyporheic zone on the phosphorus dynamics of a large gravel-bed river, Garonne River, France. *Hydrological Processes, 23*(12), 1801-1812. doi:10.1002/hyp.7319

Wallin, E. L., Johnson, T. C., Greenwood, W. J., & Zachara, J. M. (2013). Imaging high stage river-water intrusion into a contaminated aquifer along a major river corridor using 2-D time-lapse surface electrical resistivity tomography. *Water Resources Research, 49*(3), 1693-1708. doi:10.1002/wrcr.20119

Ward, J. V., & Stanford, J. A. (1993). Research needs in regulated river ecology. *Regulated Rivers: Research & Management, 8*(1-2), 205-209. doi:10.1002/rrr.3450080123

Wilcock, P. R., Kondolf, G. M., Matthews, W. V. G., & Barta, A. F. (1996). Specification of sediment maintenance flows for a large gravel-bed river. *Water Resources Research, 32*(9), 2911-2921. doi:10.1029/96wr01627

Williams, M. D., Rockhold, M., Thorne, P. D., & Chen, Y. (2008). *Three-Dimensional Groundwater Models of the 300 Area at the Hanford Site, Washington State* (PNNL-17708). Retrieved from Pacific Northwest National Laboratory, Richland, WA:

Woessner, W. W. (2000). Stream and fluvial plain groundwater interactions: Rescaling hydrogeologic thought. *Ground Water, 38*(3), 423-429. doi:10.1111/j.1745-6584.2000.tb00228.x

Wondzell, S. M. (2015). Groundwater-surface-water interactions: Perspectives on the development of the science over the last 20 years. *Freshwater Science, 34*(1), 368-376. doi:10.1086/679665

Zachara, J. M., Chen, X. Y., Murray, C., & Hammond, G. (2016). River stage influences on uranium transport in a hydrologically dynamic groundwater-surface water transition zone. *Water Resources Research, 52*(3), 1568-1590. doi:10.1002/2015WR018009

Zachara, J. M., Long, P. E., Bargar, J., Davis, J. A., Fox, P., Fredrickson, J. K., . . . Yabusaki, S. B. (2013). Persistence of uranium groundwater plumes: Contrasting mechanisms at two DOE sites in the groundwater-river interaction zone. *Journal of Contaminant Hydrology, 147*, 45-72. doi:10.1016/j.jconhyd.2013.02.001

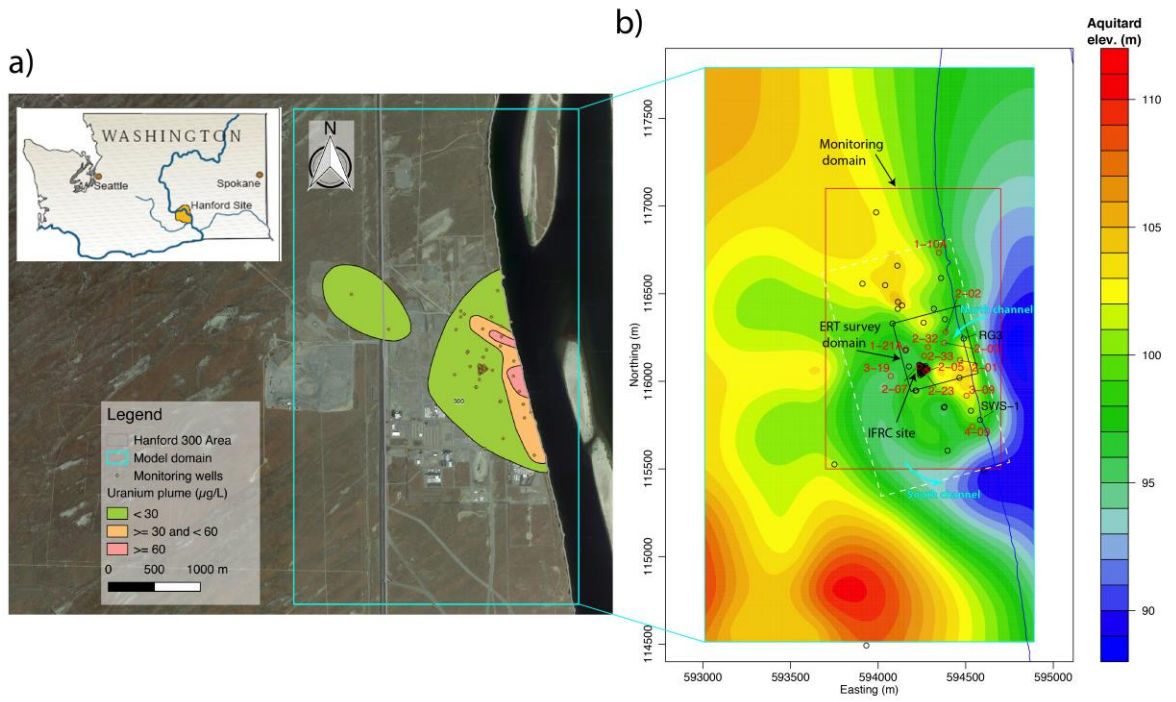

Figure 1. Study site: a) Uranium plume within Hanford's 300 Area along the Columbia River shoreline. Cyan rectangle is approximate modeling domain. b) Groundwater-surface water study site and basal aquitard topography showing the north and south channel. The land surface is at 115.6 m. Wells sampled in this study are marked with red circles. Dashed white rectangle indicates the domain where high-frequency velocity field is generated in Movie S1. A previous study (Zachara et al., 2016) focused on the IFRC site only.

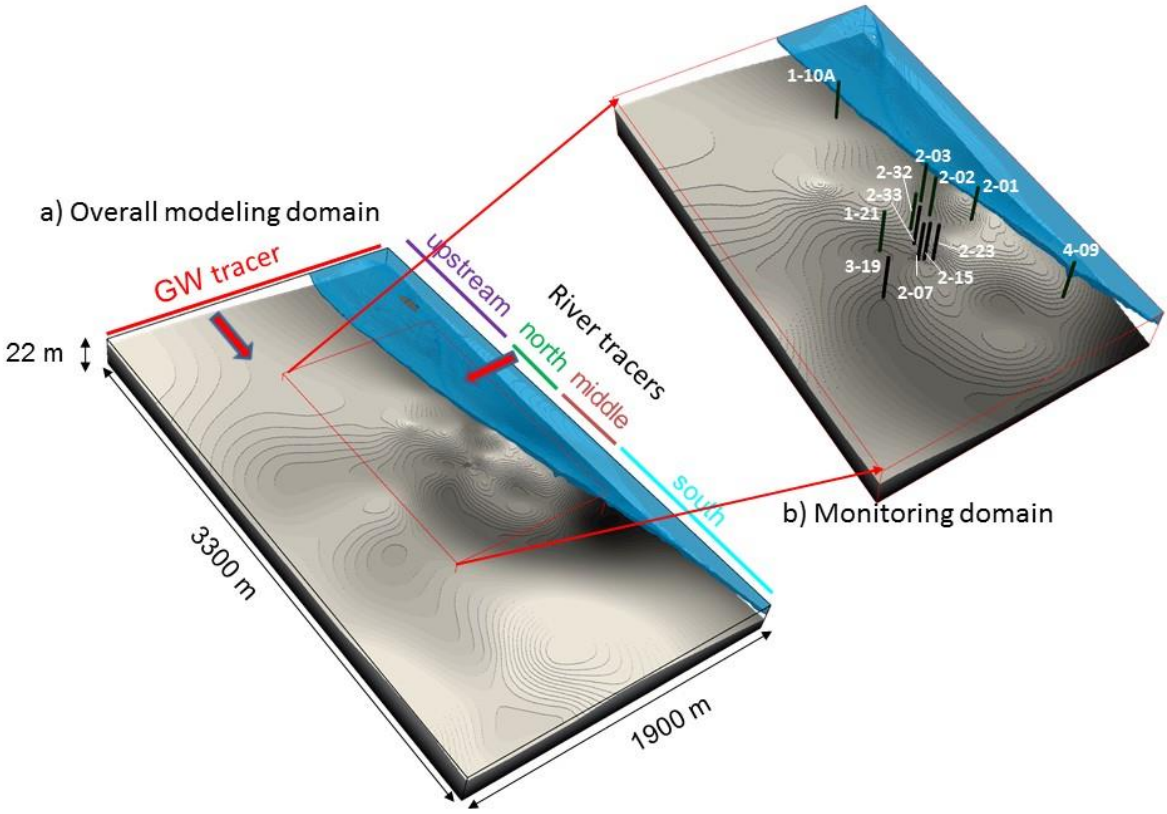

Figure 3. Zachara et al. 2019

Figure 2. PFLOTRAN modeling domain (a), in-silico tracer injection locations (groundwater and river). Contours shown for the surface of the basal aquitard which is the Hanford-Ringold contact. Monitoring domain (b) and wells monitored in the study.

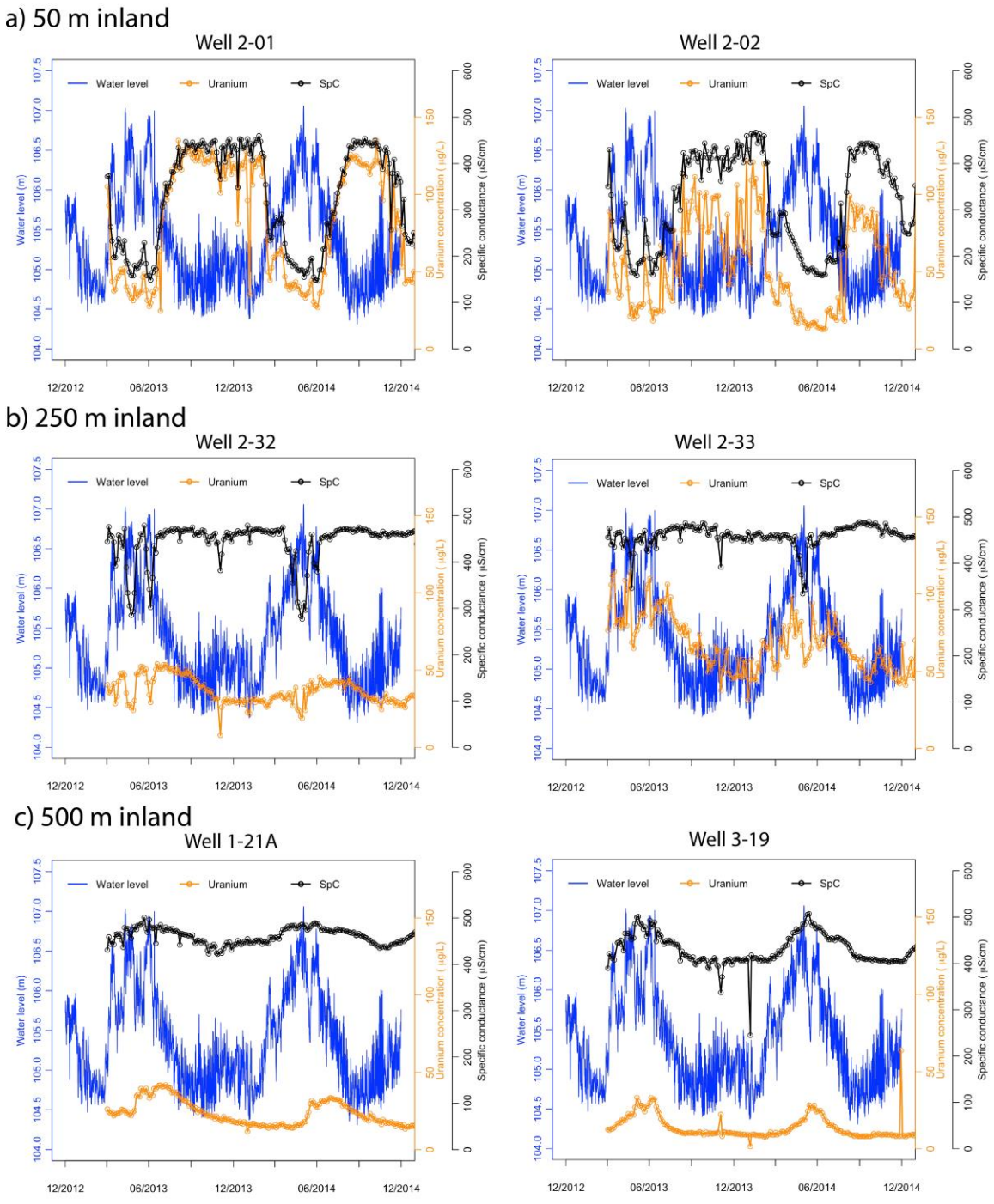

Figure 3. Well water responses to river elevation changes vary with distance from the river shoreline. Solid blue line– river surface elevation in m; black points – SpC measured in bailed samples; orange points – U_{aq} measured in bailed samples.

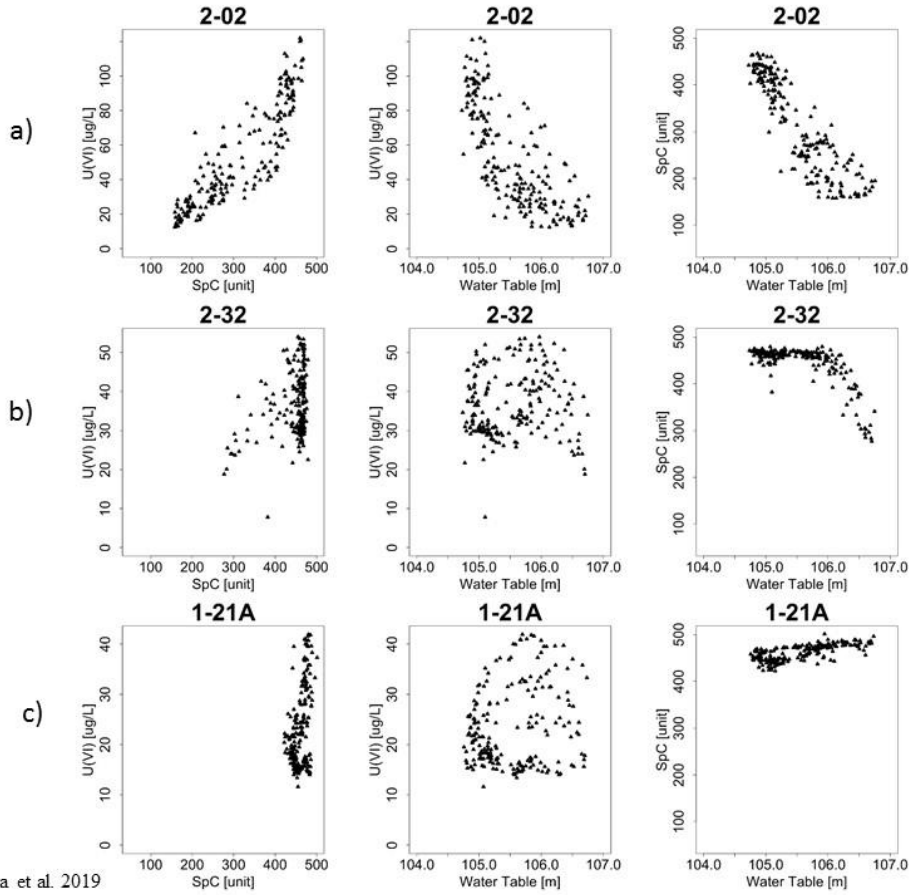

Figure 5. Zachara et al. 2019

Figure 4. Relationships between, U_{aq}, SpC, and water table elevation for representative near-shore a), intermediate distance b), and inland wells c). Plots for other wells shown in Figure S5.

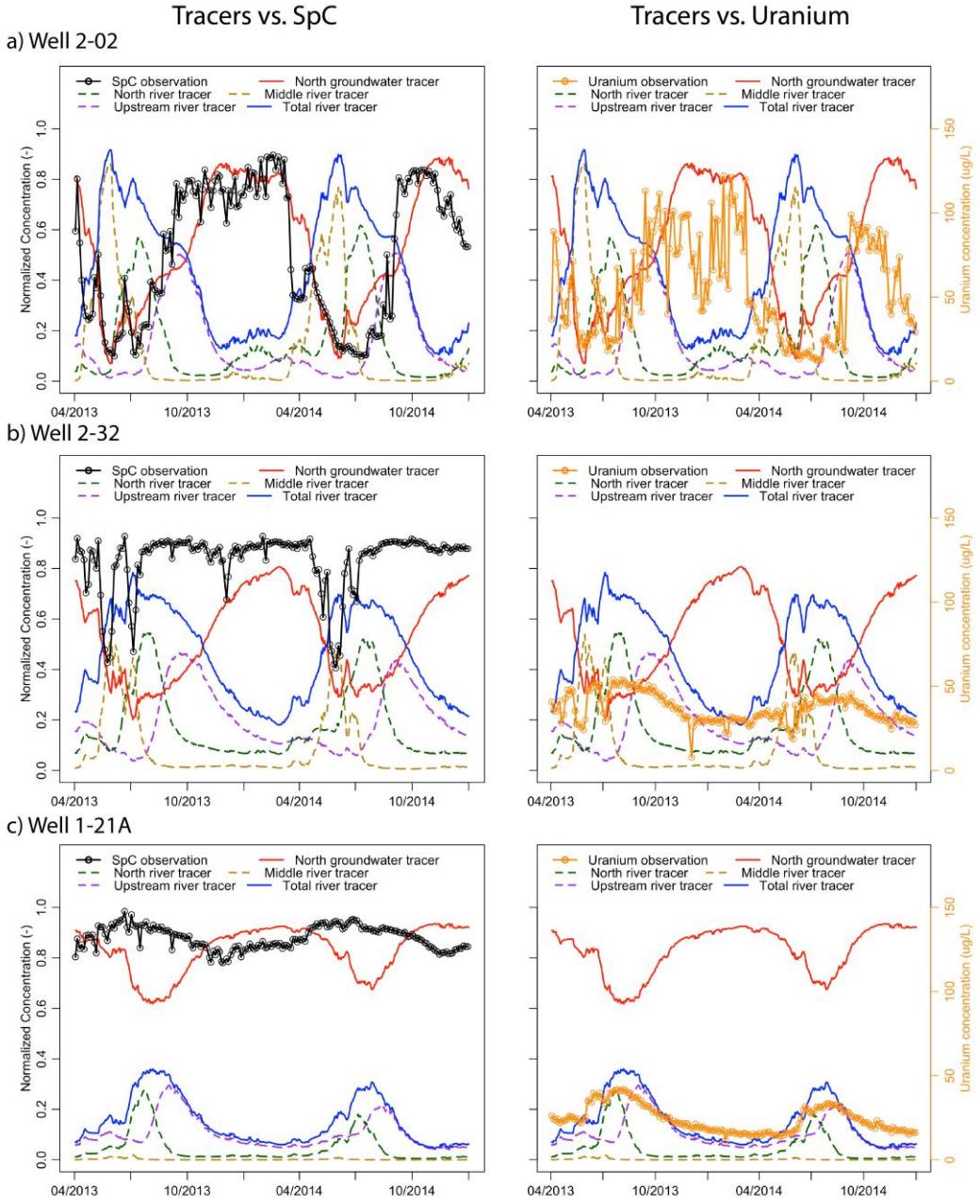

Figure 5. Simulated groundwater and river tracer breakthrough and measured SpC and U_{aq} concentrations for representative near-shore well 2-02 (a), Well 2-32 (b) and Well 1-21A (c). Black solid line with circle markers are measured SpC. Orange solid line with circle markers are measured U_{aq}. red solid line is north groundwater tracer, blue solid line is total river tracer, and other colors are as noted.

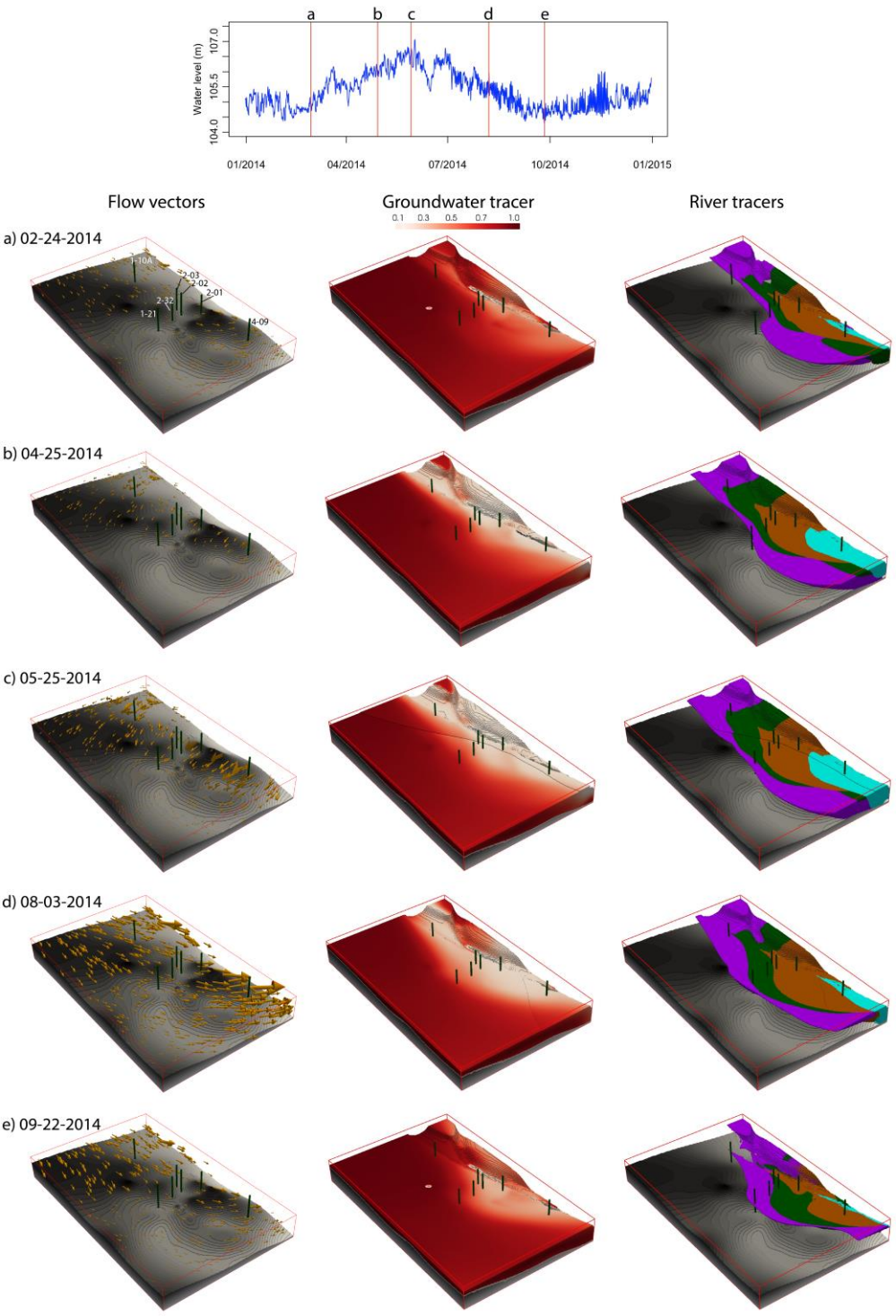

Figure 6. Groundwater flow vectors, groundwater tracer and river tracers at various river elevation, 02-24-2014 (a), ascending river elevation, 04-25-2014 (b), high river elevation, 05-25-2014 (c), descending river elevation, 08-03-2014 (d) and low river elevation after drainage of the spring pulse, 09-22-2014

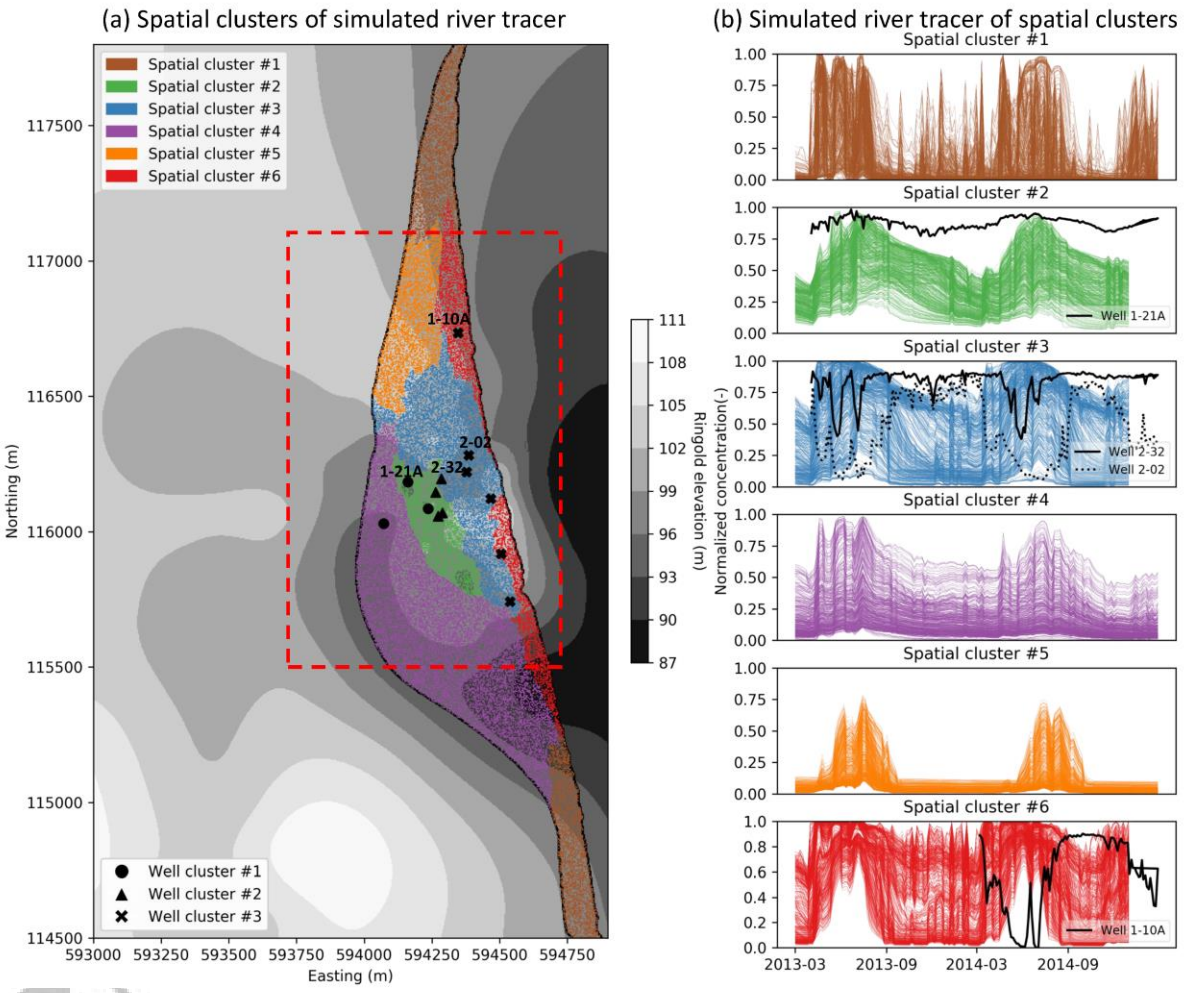

Figure 7. Spatial clustering results of simulated river tracer and measured groundwater SpC: a) the colored areas represent different spatial clusters of the simulated river tracer, black dots represent different well clusters based on SpC measurements, the grey contour represents the elevation of the low permeable Ringold sediments; b) time series of normalized river tracer of different spatial clusters. The black lines are the normalized SpC measurement of the representative wells that fell into each spatial clusters.

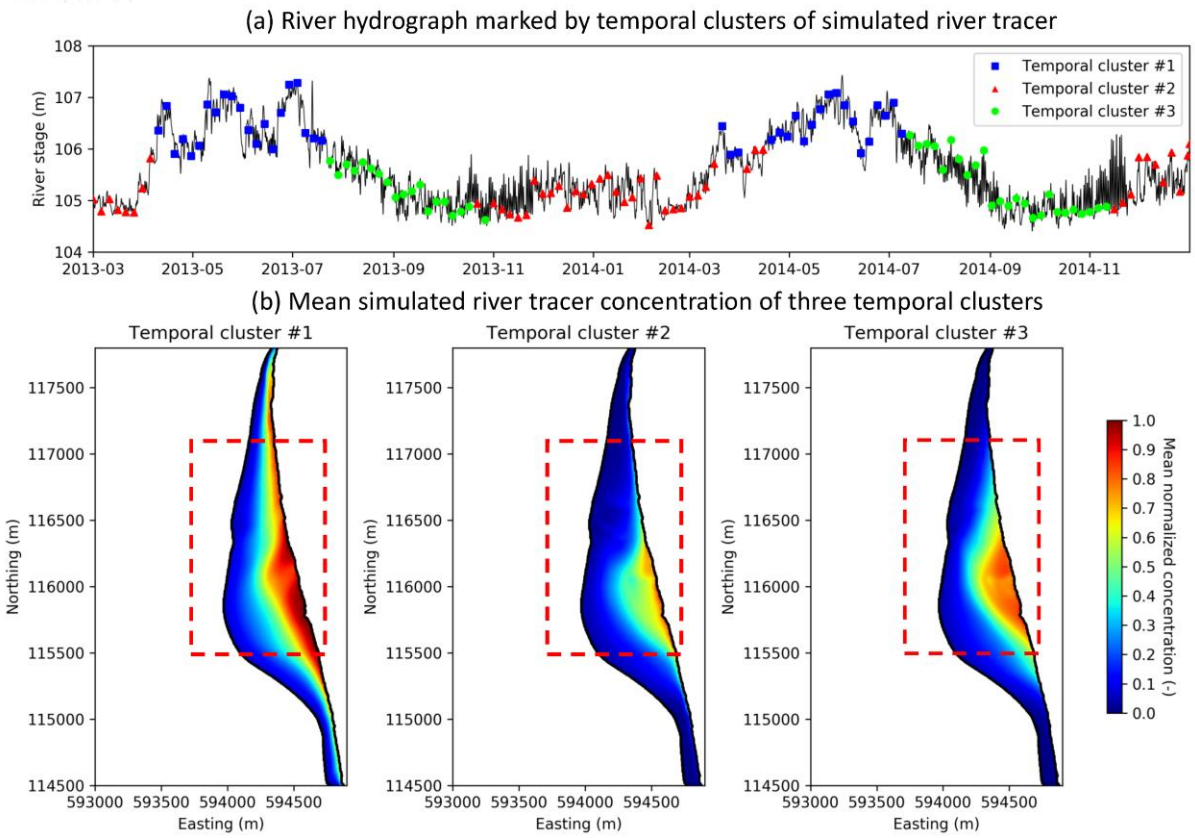

Figure 8. Temporal clustering results of simulated river tracer and measured groundwater SpC: a) river hydrograph (black line) marked by temporal clusters of simulated river tracer (colored dots), b) mean river tracer concentration of three temporal clusters.

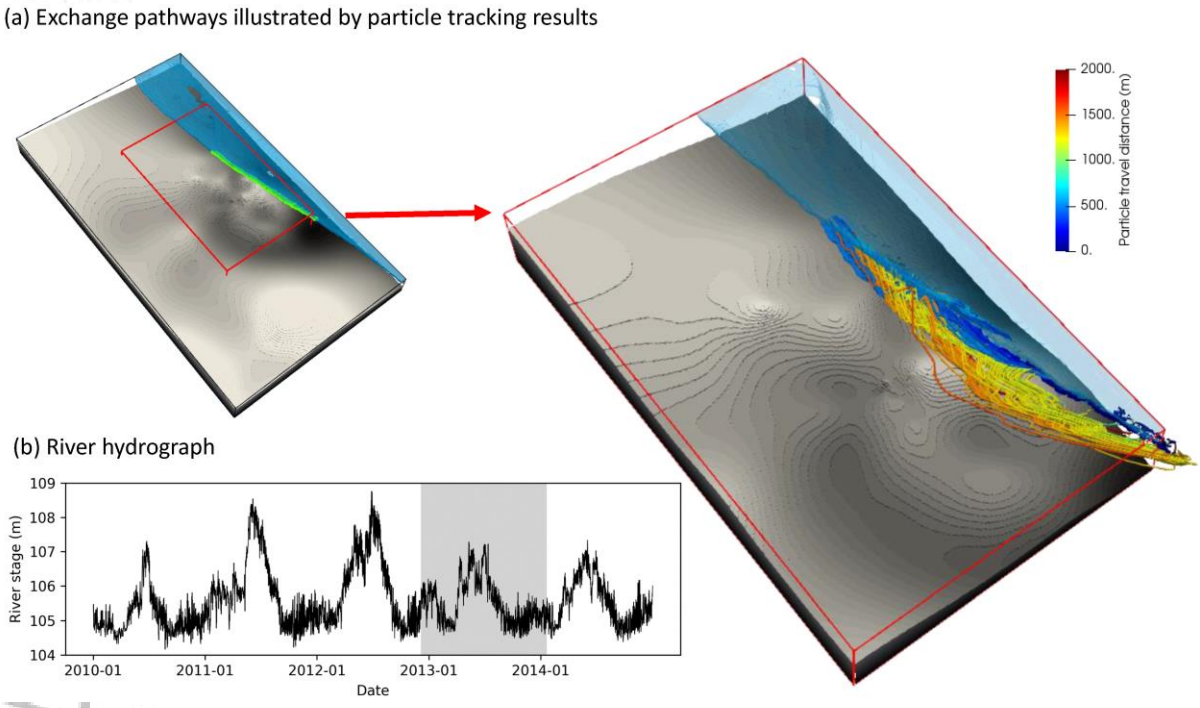

Figure 9. Hydrologic exchange pathways illustrated by particle tracking results extracted from a previous study conducted in the same site (Song et.al 2019). The green dots in the left subplot in (a) are the particle releasing location at the river-aquifer interface.The colors of exchange pathways represent particle travel distance before they returned to river. Warmer colors mean particle travel longer distance (and time) in the aquifer. The grey shadow in the river hydrograph plot (b) indicated the time duration of the particle tracking.